SIMULATION OF THE CLIMATE AT THE LAST GLACIAL MAXIMUM USING THE NCAR GLOBAL CIRCULATION MODEL

Jill Williams, R. G. Barry, and W. M. Washington

Occasional Paper No. 5

INSTITUTE OF ARCTIC AND ALPINE RESEARCH . UNIVERSITY OF COLORADO

NCAR MS. No. 2120-73-8

SIMULATION OF THE CLIMATE AT THE LAST GLACIAL MAXIMUM USING THE NCAR GLOBAL CIRCULATION MODEL

Jill Williams[1], R.G. Barry[1], and W.M. Washington[2]

[1] Institute of Arctic and Alpine Research and Department of Geography, University of Colorado, Boulder, Colorado, 80302

[2] National Center for Atmospheric Research, Boulder, Colorado, 80302

(Sponsored by the National Science Foundation)

Institute of Arctic and Alpine Research Occas. Paper No. 5

ABSTRACT

The NCAR global circulation model has been used to simulate global climatic conditions in January and July at present and at the Würm/Wisconsin glacial maximum about 20,000 BP.

The ice age simulations indicate that mean zonal wind strength in July in the middle latitudes of the Northern Hemisphere was comparable with present winter conditions. The upper westerlies were not apparently displaced south of the Laurentide ice sheet. The Icelandic and Aleutian lows in January were displaced 10° southward, the Siberian high remained unchanged from the control situation and a new low center was found over eastern Europe and the European USSR. In July the intensity of the South Asian low was reduced and high pressure developed over most of Asia. Maps of cyclone frequency in a 30-day period showed the influence of major ice sheets and sea ice in displacing zones of cyclone activity southward in January. Frequent cyclones occurred over central North America and there was a continuation of cyclone activity in the North American and Siberian Arctic. In July there were major storm tracks across the North Atlantic and from eastern Europe into Asia. There was virtually no cyclonic activity near the Laurentide Ice Sheet in July.

Cloud cover and precipitation were also analysed. Changes in precipitation for the glacial maximum cases are mainly quantitative rather than affecting its spatial distribution. The zonal averages suggest small changes for the southern hemisphere. In the northern hemisphere precipitation was decreased slightly in winter with most pronounced effects between 0-10°N and 55-70°N. The summer shows a dramatic reduction of precipitation north of 10°N.

A comparison of two January control cases indicated that slightly different boundary conditions did not greatly change the results of the simulation. There is broad agreement between these palaeoclimatological reconstructions and those of other studies using different models.

1. INTRODUCTION

Until recently, paleoclimatic reconstructions have been necessarily based on either simple analogue principles using "extreme" conditions in the meteorological record as a guide (Willett, 1950; Mather, 1954; Namias, 1957) or on diagnostic relationships between circulation features and atmospheric parameters (Flohn, 1964; Lamb et al., 1966; Lamb and Woodroffe, 1970). Numerical models of the atmospheric circulation are now sufficiently well-developed to reproduce the basic climatological characteristics of the atmosphere over the entire globe, and their application to problems of climatic variability has recently begun. For example, Shaw and Donn (1968) used Adem's thermodynamic model to examine the Milankovitch hypothesis and MacCracken (1970) assessed the influence of an open Polar Ocean using a zonally symmetric model. The assumptions of the latter models are rather restrictive, but a simulation of the circulation in July at present and at the last glacial maximum has recently been carried out by Alyea (1972) who developed a 2-level model for the northern hemisphere incorporating a realistic geography.

In the work reported here the NCAR Global Circulation Model (Kasahara and Washington, 1971) has been used to simulate the global climate for conditions in January and July at present (control cases) and at the Würm/Wisconsin glacial maximum about 20,000 BP. A previous paper (Barry, 1973) outlined some of the preliminary findings with respect to mean pressure and zonal wind averages. The present study reports more fully on the simulation results, including an examination of "synoptic" features and climatic elements, as well as comparing them with those of Lamb and Woodroffe (1970) and Alyea (1972).

2. THE MODEL

(a) Basic Features

The NCAR model has been described in detail by Kasahara and Washington (1967, 1971) and Washington and Kasahara (1970). We shall only briefly describe the version used in this paper. The model is global and employs spherical polar coordinates in the horizontal with a resolution of 5° in latitude and longitude. The longitudinal resolution is decreased near the poles to keep the geographical distances more uniform poleward of 60°. The vertical coordinate is height where the atmosphere is divided into six layers of 3 km each. The prognostic variables are longitudinal and latitudinal components of momentum ρu and ρv, pressure p, and water vapour content ρq, where q is the specific humidity. The diagnostic variables are vertical velocity w, temperature T, and density ρ. The main dynamical assumption is that the model atmosphere is hydrostatic. The resulting set of equations is commonly referred to as the primitive equation system.

The physical processes included in the model are: absorption of solar energy in the atmosphere, cooling and heating due to infra-red radiation, model-derived cloudiness at 3 and 9 km, heating due to the release of latent heat of water vapour condensation, boundary layer transfers of momentum, sensible heat and water vapour, and horizontal and vertical diffusion of momentum, sensible heat and water vapour within the model atmosphere. Over non-ocean areas, the surface temperature is computed from a surface energy balance of solar radiation, infrared radiation, sensible heat, and evaporation and heat conduction into the ground. The diurnal variation of the sun is also included. One of the limitations of this version of the model is that a Bowen ratio of unity over all non-ocean regions is assummed. Therefore, the

ratio of sensible heat flux to water vapour flux is not variable. This assumption has since been removed in later versions of the model so that soil moisture can be accounted for.

Some slight modifications from the input data of Kasahara and Washington (1971) were incorporated. The snow line is taken from Posey and Clapp (1964), as are most of the albedo values. Adjustments have been made using additional albedo data from Barry and Chambers (1966), Conover (1965), Davies (1963), Dirmhirn and Belt (1971), Kung et al. (1964), Oguntoyinbo (1970), and Stanhill et al. (1966).

(b) Ice Age Data

Modifications were made to the surface boundary conditions for January and July at the last glacial maximum by constructing base maps of ice and snow cover, sea surface temperatures, coastlines and vegetation (see Barry, 1973). Data were drawn from a wide variety of sources:

(i) sea surface isotherms for the North Atlantic are from McIntyre (1967). Ocean surface temperatures elsewhere are estimated on the basis of information given by Emiliani (1971). None of the evidence is based on oxygen isotope estimates.

(ii) the sources used to outline the horizontal and vertical extent of ice and the distribution of vegetation are shown in Table 1.

(iii) the snow line in July is assumed to be coincident with the equatorward ice margins. For January it is positioned subjectively along the reconstructed treeline or along the southern limit of steppe in view of the present day relationship between these features.

(iv) the coastline has been changed in the areas of Indonesia, Australia -

New Guinea, off Spain and off eastern North America following the interpretation of Flint (1971).

Fig. 1 shows the data grid for the oceans, continental and pack ice margins, and contours of orography or ice sheets. Fig. 2 illustrates the sea surface isotherms and generalized albedo data for the January case.

(c) Initial Conditions

The initial conditions are identical in each pair of experiments (except as described above). The experiments are started from an isothermal atmosphere at rest with the initial pressure distribution computed from the hydrostatic equation for a constant temperature. The initial specific humidity is zero. The sun's declination is set as mid-January and mid-July. The control cases used the same initial conditions as Kasahara and Washington (1971)

3. SIMULATION RESULTS

The experiment was performed for a control case (present conditions) and the glacial maximum for both January and July. The results to be discussed are in each case averages of the meteorological fields for Day 51 to Day 80. Previous investigations (Kasahara and Washington, 1971) show that computed values of global eddy kinetic energy stabilize after about 25 days with this model. Emphasis here is placed on northern hemisphere conditions.

(a) Mean Patterns

(i) Control Cases

In January and July the model simulations reproduced most features of the observed atmospheric circulation. For the MSL pressure simulation, comparisons are made with the mean maps of Crutcher and Meserve (1970). It is, of course, evident that the model results may more nearly resemble a particular month rather than the long-term mean condition. In January the model produces

a separate low pressure cell at 130°E along the Siberian coast while the Aleutian low is poorly represented (Fig. 3). This was also the case with Kasahara and Washington's (1971) January experiment. The Azores-North African high is displaced to the western Mediterranean and the Siberian center is displaced southeastward compared with the observed mean. For July (Fig. 4) the discrepancies with the model simulation are rather minor. They pertain to the westward extension of the Asian low pressure area across North Africa and the Mediterranean, instead of the Azores anticyclone extending eastward, and the excessive intensity of the small high pressure area over the northern North Atlantic.

The computed zonal westerly maxima are located at too high an altitude in both months (Figs. 5(a) and 6(a)) which seems to be due to the upper boundary conditions in the model (Kasahara and Washington, 1971). The northern hemisphere jet is correctly located in January, but in July it is shown too far north (Newell et al., 1970). The computed southern hemisphere maximum is correctly located in July but is a little equatorward of its observed position in January (Newton, 1972). The equatorial easterlies are correctly shown in July but in January the computed ones extend only to 700 mb.

A zonal profile at the 7.5 km level (Fig. 7) provides a further measure of the representation of observed features in the simulation. The observed mean maximum at the 400-mb level at 25°-30°N in January is replaced in the simulation by a much broader feature, while the southern hemisphere maximum is shown some 5°-10° too far equatorward. More important, the observed equatorial easterlies are missed. In the July case the northern hemisphere maximum is barely represented and again equatorial easterlies do not feature

in the simulation, although a minimum of westerlies is indicated.

The patterns of simulated climatic elements are evaluated briefly in section 3(c).

(ii) Glacial Maximum

For the northern hemisphere at the glacial maximum the zonal wind profile in January shows a reduced westerly maximum shifted 5° poleward compared with the present (Fig. 5(b)) whereas in July (Fig. 6(b)) it is stronger than at present and displaced equatorward to 45°N. However, interpretation of the latter change is complicated by the discrepancy referred to in the July control case. The changes below the jet stream level are somewhat different. At 4.5 km (ca. 580 mb) the zonal wind in January is stronger than at present at 45°-50°N. In July there is no difference from present in the tropics but the zonal wind strength is almost comparable with present winter conditons in middle latitudes.

Careful interpretation of the MSL pressure maps is necessary since the evaluation of MSL pressure assumes a constant temperature below the land or continental ice sheet surface which is equal to the mean temperature of the overlying layer (Kasahara and Washington, 1971, p. 659). This assumption makes the computed MSL pressures rather too high.

Fig. 8 shows a 10° southward displacement of the Icelandic and Aleutian lows in January while the Siberian high remains unchanged from the control case. However, a new low center is indicated over eastern Europe and the European USSR. The MSL high over northern Canada is essentially fictitious but the small low off the east coast should be noted. Changes are slight in the tropics although the low centers over the southern hemisphere continents are shifted 5°-10° equatorward.

In July (Fig. 9) the most striking feature is the reduced intensity of the south Asian low and the development of high pressure over most of Asia. The Aleutian low resembles the observed winter pattern at present. High pressure dominates the eastern North Atlantic and North American sectors although the latter feature is fictitious for most of Canada. Compared with the control case there is a weak but nearly continuous belt of equatorial low pressure.

(b) Disturbances

The synoptic activity has been examined by preparing maps of the frequency of cyclone and anticyclone centers on Days 51-80 of each of the four cases (Figs. 10 and 11). Results for the control cases have compared with those of Klein (1957) and Taljaard (1972). It has not yet proved possible to trace the movement of cyclones unambiguously, so that depression tracks can only be inferred.

For January, the major omissions are the cyclonic activity over the Mediterranean and mid-western North America. The lows in the eastern North Pacific and those of the southern hemisphere westerlies are shown too far equatorward. For July, the map of disturbance activity is considerably less satisfactory than the mean patterns. Disturbances are wholly unrepresented in the mean monsoon low, probably because they are subgrid-scale features, while those shown over the Mediterranean and extreme eastern Asia are too far north.

The glacial maximum map for January clearly shows the influence of the major ice sheets and sea ice in displacing the zones of cyclonic activity southward. The pattern bears a strong similarity to an early reconstruction by Bryan and Cady (1934). Additionally, several features are indicated which are not apparent in the mean pressure maps. In particular, there are frequent

cyclones over the central United States and there is a continuation of some disturbance activity in the North American and Siberian Arctic. Other major changes from the control case are the big reductions in frequency of cyclones over the western Indian Ocean, the central equatorial Pacific and over Australia. The subtropical anticyclones in both hemispheres show fewer centers although the cyclone "track" in the southern westerlies is displaced poleward in the South Atlantic and South Pacific oceans.

The July glacial pattern has several striking features. There is a major storm track across the North Atlantic to west of Ireland and a continuation of this, or a further major track from eastern Europe into Asia. Another prominent area of cyclonic activity is the Aleutians. In contrast with January, there is virtually no cyclonic activity in the vicinity of the Laurentide ice sheet. The equatorial Pacific shows frequent cyclonic activity in July at the glacial maximum and an additional "zone" of cyclones is interposed at about 35°S on the equatorward side of the weakened subtropical highs. In the South Atlantic and South Pacific the distributions suggest blocking patterns and there is apparently less synoptic activity in the southern westerlies.

(c) Climatic Elements

Cloudiness. The computed zonal mean cloudiness at 3 km for July (Fig. 12) compares quite well with the observed data on total cloudiness for the northern hemisphere given by London (1957), but in January the computed values are larger than observed in middle and high latitudes and show a minimum rather than a maximum at 5°-10°N. However, cloudiness data recently computed by Schutz and Gates (1971) incorporating satellite observations show a much better fit with the model in this zone, and this serves to demonstrate the present problems

in verifying simulation results. For the southern hemisphere the agreement between the control case and Van Loon's (1972a)data is satisfactory in January when an allowance of 5-10% is made for high cloud, but in July the computed values are too large between 35°-55°S and are probably too low for 0°-20°S and 75°-90°S even when allowance is made for high clouds. The changes between the control cases and the glacial maximum (Fig. 12) indicate in July at glacial maximum considerably more cloud cover poleward of 25°N, and in January a similar increase in the subtropics but with a decrease from 50°-70°N.

Precipitation. The zonal means of 90-day precipitation (Fig. 13) show that, in comparison with Möller's (1951) estimates, the computed values for the control cases are too large by a factor of 2-5. However, it is worth noting Tucker's (1961) maps show more precipitation than Möller's in high-middle latitudes over the North Atlantic Ocean. The zonal distribution is fairly well represented in July although the maximum in mid-latitudes of the southern hemisphere is 10° equatorward of its observed position. The peak at 60° can probably be discounted since inter-annual variations in precipitation may be quite large. The January control case shows excessive precipitation in the equatorial trough and no zonal subtropical minimum in the southern hemisphere. These discrepancies indicate either that the precipitation processes in the model are too efficient and/or that climatic data on equatorial precipitation are too low.

Study of the geographical distribution of precipitation shows that many of the differences between the observed and control case zonal averages are caused by local areas of anomalously high or low precipitation in the simulation. The geographical distribution of precipitation in the January control case and the data for December-February of Möller (1951) show good

agreement. Our map is almost identical with that of Kasahara and Washington (1971, Fig. 9(b)). In subtropical areas there is a more meridional pattern of high and low precipitation zones in the control case. Between 0° and 20°S from 160°E eastward to 140°W, over South Africa and South America there are areas of heavy precipitation, which are correctly located according to Möller's map, but have excessive amounts. Also, in the Indian Ocean in the same latitude belt there is an area of high precipitation in the January control case not present in the observed data. The agreement in July between the computed and observed geographical distributions is not as good. The observed pattern in the southern hemisphere shows less zonality than the simulation, the observed maximum over the Amazon basin is missing, and one shown north of the Sahara is not seen in Möller's map. In the tropical Pacific, particularly in the east, and the Asian monsoon area (40°-160°E) the computed values are too large.

The ice age zonal averages (Fig. 13) suggest for the southern hemisphere a negligible change in overall summer conditions and only a slight decrease in middle latitudes in winter. In the northern hemisphere precipitation is decreased slightly in winter with the most pronounced effects between 0°-10°N and 55°-70°N. The summer season shows a dramatic reduction north of 10°N, by 50% at 20°N and by 75% north of 60°N compared with the control case.

Examination of the geographical distributions indicates that the changes for the ice age cases are mainly quantitative rather than qualitative. The major changes in distribution are in the North Atlantic area where, in January at glacial maximum, the maximum precipitation is shown to be displaced to the southwest of the British Isles. In July the maximum follows the zone of frequent cyclonic activity across the Atlantic shown in Fig. 11(b). There

is even less precipitation in the subtropical arid zones in the glacial maximum January and July than in the control cases and the Asian summer monsoon is reduced in intensity while over east and northeast Asia the maxima of the July control case are virtually eliminated. An area of low precipitation off the California coast in the July control is replaced by one of high precipitation at the glacial maximum.

4 JANUARY CASES WITH SLIGHTLY DIFFERENT BOUNDARY CONDITIONS

The January control case (case 165) has been compared with another January simulation (case 156)(Kasahara and Washington, 1971) which had different albedo values and different extent of northern hemisphere pack ice. The differences are not large, but comparison of the 30-day means produced by the two simulations gives some indication of the sensitivity of the model to small changes in boundary conditions.

Of the maps studied, the sea-level pressure maps show the greatest differences between the two cases. In case 156 the Icelandic low is farther southwest and the Aleutian low, although displaced south from the observed position, is shown. Over Europe there is a low pressure center in case 156, with high pressure over the Eurasian Arctic; in the case 165 there is low pressure in the Eurasian Arctic resulting in a stronger pressure gradient between the equator and the north pole than is seen in case 156. The surface pressures over the southern hemisphere, North America, the Mediterranean area and North Africa are not significantly different between the two cases.

Maps of the vertical wind velocity near the surface and 1.5 km show little difference between the two cases, except that there is an area of greater subsidence over North America between 40°N and 60°N in case 165. Maps of low clouds and ground temperature for both models show similar geographical

distributions and magnitudes. The geographical distributions of precipitation are also similar and a plot of the zonal averages of precipitation in case 156 shows that there is no difference in this respect between the models in the southern hemisphere, while in the northern hemisphere the peak at 60°N found in the January control case (see Fig. 13) does not occur in case 156 and the peaks at 35°N and 5°N are less pronounced.

The only major difference between the models found in the comparisons made so far are in sea-level pressure and precipitation in the northern hemisphere. A comparison of the energy and momentum budgets might show significant results of changes in forcing, but at present it is concluded that small changes in the boundary conditions do not greatly change the results of the simulation.

5 COMPARISON WITH OTHER PALAEOCLIMATIC RECONSTRUCTIONS

Lamb and Woodroffe (1970), using values for summer and winter temperature derived from paleobotanical and oceanographic research for the maximum of the last ice age, obtained estimates of upper air temperature and 1000-500 mb thickness distribution over the northern hemisphere. Regions of recurrent cyclonic and anticyclonic development were then calculated and the probable prevailing surface pressure patterns were derived.

Lamb and Woodroffe suggested that the thermal pattern over the northern hemisphere in the presence of ice must have displaced the main flow of the upper westerlies into a course south of the ice. Meridional cross-sections of the zonal wind at 75°W in this study indicated that in both January and July the upper westerlies were not forced south to skirt the Laurentide ice sheet. The main flow of the upper westerlies did not, as Lamb and Woodroffe suggested, attain lowest latitude as it passed the ice dome; instead the core

of the westerlies seems to have been about 50°N over the North American ice.

The broad pattern of the circumpolar vortex (as evidenced by 6km pressure maps not included) agrees well with their inferred 1000-500 mb thickness field. However, the results indicate that cyclones frequently travelled northeastward across the Atlantic in January and July with the polar anticyclone not extending south of 60°N in the mean picture. In contrast to Lamb and Woodroffe, we find that there are marked seasonal changes of vigour and latitude of the main circulation features. For example, the Icelandic low is strong and in a southerly position during the glacial maximum in January and is replaced by a weak trough in July. Over Asia pressure systems are much stronger in January than July. In agreement with their results, we found a cyclonic regime over western Siberia, in summer and winter, during the glacial maximum. However, we found no significant seasonal shift of cyclonic activity over Europe. Over North America, the seasonal change is weak in the mean pressure fields, but there is an important locus of cyclonicity over the midwest in January.

Alyea (1972) developed a 2-level, quasi-geostrophic, spectral general circulation model in order to simulate the climate of the last glacial maximum. The model was integrated forward in time for 60 days for two experiments, a simulation of July present and July ice age conditions. Results of Alyea's model compare favourably with results of this study. Alyea found that transient eddy activity in his present day July simulation was considerably less than in the ice age case across the North Atlantic and in the regions of south-central to eastern Europe; he also found that a large number of cyclone waves under the influence of strong steering currents were drawn across the

Scandinavian ice sheet. However, he found a relatively small number of travelling waves across North America during July and suggested that possibly the winter circulation was able to supply enough moisture to maintain the ice sheet. This is confirmed by our results (Fig. 10(b)). As in this study, and that of Lamb and Woodroffe, Alyea found that the circumpolar vortex was displaced southward, although he indicates that it was centered south of Greenland.

6 CONCLUSIONS

The broad agreement between the palaeoclimatological reconstructions and those of other studies using quite different models implies that such simulations will greatly augment our understanding of past climatic patterns. The preliminary tests with slightly different boundary conditions indicate that the model is not unduly sensitive to such minor changes. This lends confidence to the interpretation of the results as approximating the long-term mean conditions. While many regional features remain to be checked or corrected the essential features of the northern hemisphere circulation at the last glacial maximum can, with reasonable confidence, be characterized as follows:

1. Mean zonal wind strength in July in mid-latitudes of the northern hemisphere was comparable with present winter conditions. The upper westerlies were not apparently displaced south of the Laurentide ice sheet.

2. The mean subpolar MSL lows were displaced 10° southward in January with a new center over eastern Europe and the eastern USSR while in July western Europe and central Asia were dominated by high pressure and the mean monsoon low was weaker than at present.

3. Cyclonic activity was displaced southward in January and July by land and sea ice with the main activity south of the Laurentide ice sheet being in

winter. Cyclones from the North Atlantic and/or Europe skirt south of the Scandinavian ice sheet into Asia at both seasons.

4. Changes in precipitation at the glacial maximum are indicated as being principally quantitative. In summer precipitation was apparently much reduced over southern and eastern Asia in the subtropical arid zones and north of 10°N. In winter, precipitation amounts were similar to present day, but with slight reductions in the northern hemisphere and in southern hemisphere middle latitudes.

Analysis of the energy, momentum and moisture budgets for the various simulations will be carried out in the near future. Application of the reconstructed surface wind fields to models of ocean surface dynamics would also be of value. Among other things, this would provide a check on the sea surface isotherm patterns. Ultimately, a model incorporating oceanic circulations will be required.

ACKNOWLEDGEMENTS

We would like to thank Gloria Williamson of NCAR for supervising the running of the model and the NCAR computing facility for their support (NCAR is sponsored by the National Science Foundation). We would also like to thank Kathleen Brenton and Gerald Meehl for preparing the figures. Jill Williams is supported by a fellowship from the University of Colorado.

REFERENCES

Alyea, F. N. 1972 'Numerical simulation of an ice age paleoclimate,' Atmos. Sci. Pap., No. 193, Colorado State University, 120 pp.

Barry, R. G. 1973 'The conditions favoring glacierization and deglacierization in North America from a climatological viewpoint,' Arct. Alp. Res. 5, in press.

Barry, R. G. and Chambers, R. E. 1966 'A preliminary map of summer albedo over England and Wales', Quart. J. R. Met. Soc. 92, pp. 543-548.

Bigarella, J. J. and Andrade, G. O. de 1965 'Contribution to the study of the Brazilian Quaternary', Geol. Soc. Amer. Spec. Paper, no. 84, pp. 433-451.

Bonatti, E. 1966 'North Mediterranean climate during the last Würm glaciation', Nature, 209, pp. 984-985.

Bryan, K. and Cady, R. C. 1934 'Pleistocene climate of Bermuda', Amer. J. Sci., 227, pp. 241-64.

Butzer, K. W. 1971 Environment and archeology: an ecological approach to prehistory, 2nd ed. Aldine-Atherton, Chicago, 703 pp.

Conover, J. H. 1965 'Cloud and terrestrial albedo determinations from TIROS satellite pictures', J. Appl. Met., 4 pp. 378-386.

Coope, A. R., Morgan, A. and Osborne, P. J. 1971 'Fossil Coloeprera as indicators of climatic fluctuations during the last glaciation in Britain', Palaeogeog., Palaeoclim., Palaeoecol., 10, pp. 87-101.

Crutcher, H. L. and Meserve, J. M. 1970 'Selected level heights, temperatures and dew points for the Northern Hemisphere', NAVAIR 50-1C-52 Revised, Naval Weather Service Command, Washington, D.C.

Damuth, J. E. and Fairbridge, R. W. 1970 'Equatorial Atlantic deep sea arkosic sands and ice age aridity in tropical South America', Geol. Soc. Amer. Bull., 81, pp. 189-206.

Davies, J. A. 1963 'Albedo investigations in Labrador-Ungava' Archiv. für Met., Geophysik und Biokl., Ser. B, 13, pp. 137-151.

Dirmhirn, I. and Belt, G. H. 1971 'Variation of albedo of selected

sagebrush range in the intermountain region', Agric. Met., 9, pp. 51-61.

Emiliani, C. 1971 'The Amplitude of Pleistocene climatic cycles at low latitudes and the isotopic composition of glacial ice', in Late Cenozoic Glacial Ages, Yale Univ. Press, ed. K. K. Turekian, pp. 183-197.

Fairbridge, R. W. 1961 'Convergence of evidence on climatic change and ice ages', Ann. N.Y. Acad. Sci., 96, pp. 542-579.

Fairbridge, R. W. 1970 'World paleoclimatology of the Quaternary', Revue de géog. phys. et géol. dynam., 12, pp. 97-104.

Flint, R. F. 1971 Glacial and Quaternary Geology, J. Wiley and Sons, New York, 892 pp.

Flohn, H. 1964 'Grundfragen der Paläoklimatologie im Lichte einer theoretischen Klimatologie', Geol. Rund., 54, pp. 504-575.

Frenzel, B. 1968 'The Pleistocene vegetation of North Eurasia', Science, 161, pp. 637-648.

Galloway, R. W. 1965 'Late Quaternary climates in Australia', J. Geol., 73, pp. 603-618.

Gerasimov, I. P. 1969 'Degradation of the last European ice sheet', in Quaternary geology and climate, ed. H. E. Wright, National Academy of Sciences, Washington, pp. 72-78.

Grichuk, V. P. 1971 'The analysis of zonal structure of the Pleistocene vegetational cover across USSR', Pollen et Spores, 3, pp. 101-116.

Hammen, T., van der 1961 'The Quaternary climatic changes of Northern South America', Ann. N.Y. Acad. Sci., 95, pp. 676-683.

Hammen, T. van der, Wijmstra, T. A. and Molen, W. H. vander 1965 'Palynological study of a very thick peat section in Greece and the Wurm-glacial vegetation in the Mediterranean region', Geol. en Mijnbouw, 44, pp. 37-39.

Hollin, J. 1962 'On the glacial history of Antarctica', J. Glaciol., 4, pp. 173-195.

Holtedahl, H. 1967 'Notes on the formation of fjords and fjord valleys', Geograf. Annaler, 49, ser. A, pp. 188-203.

Jackli, H. C. A. 1965 'Pleistocene glaciation of the Swiss Alps and

signs of post-glacial differential uplift', Geol. Soc. Amer. Spec. Paper, no. 84, pp. 153-157.

Kaiser, K. 1969 'The climate of Europe during the Quaternary ice age', in Quaternary geology and climate, ed. H. E. Wright National Academy of Sciences, Washington, pp. 10-37.

Kasahara, A. and Washington, W. M. 1967 'NCAR global general circulation model of the atmosphere', Mon. Wea. Rev., 95, pp. 389-402.

Kasahara, A. and Washington, W. M. 1971 'General circulation experiments with a six-layer NCAR model, including orography, cloudiness and surface temperature calculations', J. Atmos. Sci., 28, pp. 657-701.

Klein, W. H. 1957 'Principal tracks and mean frequencies of cyclones and anticyclones in the Northern Hemisphere', Research Paper No. 40, Weather Bureau (Washington), 60 pp.

Kung, E. C., Bryson, R. A., Lenschow, D. H. 1964 'Study of a continental surface albedo on the basis of flight measurements and structure of the earth's surface cover over North America' Mon. Wea. Rev., 92, pp. 543-564.

Lamb, H. H., Lewis, R. P. W., and Woodroffe, A. 1966 'Atmospheric circulation and the main climatic variables between 8000-OBC: meteorological evidence', Proceedings of the International Symposium on world climate 8000-OBC, Royal Met. Soc., London, pp. 174-217.

Lamb, H. H. and Woodroffe, A. 1970 'Atmospheric circulation during the last ice age', Quat. Res., 1, pp. 29-58.

London, J. 1957 'A study of the atmospheric heat balance', Final Rept. Contract AF 19(122)-165, Dept. of Meteorology and Oceanography, New York University (ASTIA No. 117227).

MacCracken, M. D. 1970 'Test of ice age theories using a zonal atmospheric model', Lawrence Radiation Laboratory UCRL-72803, Livermore, Calif., 58 pp.

Mather, J. R. 1954 'The present climatic fluctuation and its bearing on a reconstruction of Pleistocene climatic conditions', Tellus, 6, pp. 287-301.

McIntyre, A. 1967 'Coccoliths as paleoclimatic indicators of Pleistocene glaciations', Science, 158, pp. 1314-1317.

Möller, F. 1951 'Vierteljahrskarten des Niederschlags für die ganze Erde' Petermann's Geograph. Mitt., 95, pp. 1-7.

Namias, J. 1957 'Seasonal interactions between the North Pacific Ocean and the atmosphere during the 1960's', Mon. Wea. Rev., 97, pp. 173-192.

Newell, R. E., Vincent, D. G., Dopplick, T, G., Ferruza, D. and Kidson, J. W. 1970 'The energy balance of the global atmosphere', The Global Circulation of the Atmosphere, ed. G. A. Corby, Roy. Met. Soc., pp. 42-90.

Newton, C. W. (ed.) 1972 'Meteorology of the Southern Hemisphere', Met. Monogr., 13(35), 263 pp.

Oguntoyinbo, J. S. 1970 'Reflection coefficient of natural vegetation, crops and urban surfaces in Nigeria', Quart. J. R. Met. Soc., 96, pp. 430-441.

Oort, A. H. and Rasmusson, E. M. 1971 'Atmospheric circulation statistics', NOAA Prof. Paper no. 5, U.S. Dept. of Commerce, Rockville, 323 pp.

Polanski, J. 1965 'The maximum glaciation in the Argentine cordillera', Geol. Soc. Amer. Spec. Paper, no. 84, pp. 453-472.

Posey, J. W. and Clapp, P. F. 1964 'Global distribution of normal surface albedo', Geof. Int., 4, pp. 33-48.

Robin, G. de Q. 1964 'Glaciology', Endeavour, 23(9), pp. 102-107.

Robin, G. de Q. 1966 'Origin of the ice ages', Science J., pp. 3-8.

Schutz, C. and Gates, W. L. 1971 'Global climatic data for surface, 800 mb, 400 mb: January', R-915-ARPA. The Rand Corporation, California, 173 pp.

Shaw, D. M. and Donn, W. L. 1968 'Milankovitch radiation variations: a quantitative evaluation', Science, 162, pp. 1270-1272.

Stanhill, G., Hofstede, G. F. and Kalma, J. D. 1966 'Radiation balance of natural and agricultural vegetation', Quart. J. R. Met. Soc., 92, pp. 128-140.

Taljaard, J. J. 1972 'Synoptic Meteorology of the southern hemisphere', Met. Monogr., 13(35), pp. 139-214.

Tsukada, M. 1966 'Late Pleistocene vegetation and climate in Taiwan (Formosa)', Nat. Acad. Sci. (U.S.) Proc., 55, pp. 543-548.

Tucker, G. B. 1961 'Precipitation over the North Atlantic Ocean', Quart. J. R. Met. Soc., 87, pp. 147-158.

Van Andel, T.H., Heath, G.R., Moore, T.C. and McGeary, D.F.R., 1967, 1967, 'Late Quaternary history, climate and oceanography of the Timor Sea, Northwestern Australia', Amer. J. Sci., 265, pp. 737-758.

Van Loon, H. 1972 'Wind in the Southern Hemisphere', Met. Monogr., 13(35), pp. 87-100.

Van Loon, H. 1972b 'Cloudiness and precipitation in the Southern Hemisphere', Met Monogr., 13(35), pp. 101-112.

Wardle, P. 1964 'Evolution and distribution of the New Zealand flora, as affected by Quaternary climates', New Zealand J. Bot., 1, pp. 3-17.

Washington, W.M. and Kasahara, A. 1970 'A January simulation experiment with the two-layer version of the NCAR global circulation model', Mon. Wea. Rev., 98, pp. 559-580.

Willett, H.C. 1950 'The general circulation at the last (Würm) glacial maximum', Geograf. Annaler, 32, pp. 179-187.

Zonneveld, J.S. 1968 'Quaternary climatic changes in the Caribbean and Northern South America', Eiszeitalter und Gegenwart, 19, pp. 203-208.

Table 1. Sources of information on ice cover and vegetation at the last glacial maximum used in the experiment

Area	Ice Cover	Vegetation
N. America	Extent Flint (1971) J.D. Ives (pers. comm. 1971) J.T. Hollin (pers. co-m. 1971) Thickness J.D. Ives (pers. comm. 1971) J.T. Andrews (pers. comm. 1971) J.T. Hollin (pers. comm. 1971)	Flint (1971) Butzer (1971)
S. America	Extent and thickness Flint (1971)	Polanski (1965), Flint (1971), Bigarella and Andrade (1965), Damuth and Fairbridge (1970), Zonneveld (1968), Van der Hammen (1961)
Eurasia	Extent Flint (1971), Butzer (1971) Gerasimov (1965) Thickness Flint (1971), Butzer (1971), Robin (1964, 1966), Jäckli (1965) Holtedahl (1967)	Frenzel (1968) Bonatti (1966) Kaiser (1969) Van der Hammen et al. (1965) Grichuk (1971) Coope et al. (1971), Tsukada (1966)
Africa		Butzer (1971), Flint (1971)
Australia New Zealand	Flint (1971), Galloway (1965)	Galloway (1965), Van Andel et al. (1967) Wardle (1964), Flint (1971), Fairbridge (1970)
Antarctica	Extent and thickness Hollin (1962 and pers. comm. 1971) Pack ice extent Fairbridge (1961)	
Arctic	Pack ice extent Flint (1971)	

FIGURE CAPTIONS

Figure 1 Outline of continents, ocean grid and orography used in January and July ice age simulations. Contours shown are: dashed line, 1 km; solid line, 2km; dotted line, 4 km.

Figure 2 Albedos and sea surface temperatures used in January ice age simulation. Isotherms in °C. Dashed line is snowline. Albedos shown are: dotted, 61-100%; cross-hatched, 41-60%; broken-hatched, 21-40%; solid-hatched, 1-20%.

Figure 3 30-day mean pressure at sea-level for the January control case. Areas above 1.5 km outlined by dashed line.

Figure 4 30-day mean pressure at sea level for the July control case. Areas above 1.5 km outlined by dashed line.

Figure 5 (a) Latitude-height distribution of 30-day mean zonal wind component computed for January control case (units: m s^{-1}).

Figure 5 (b) Latitude-height distribution of 30-day mean zonal wind component computed for January ice age case (units: m s^{-1}).

Figure 6 (a) Latitude-height distribution of 30-day mean zonal wind component computed for July control case (units: m s^{-1}).

Figure 6 (b) Latitude-height distribution of 30-day mean zonal wind component computed for July ice-age case (units: m s^{-1}).

Figure 7 Latitudinal distributions of the zonal averages of the zonal wind component at 7.5 km for all cases. Observed data from Oort and Rasmusson (1971) and Van Loon (1972a).

Figure 8 30-day mean pressure (mb) at sea-level for the January ice age case. Areas above 1.5 km outlined by dashed line.

Figure 9 30-day mean pressure (mb) at sea-level for the July ice age case.

Areas above 1.5 km outlined by dashed line.

Figure 10(a) Frequency of cyclone and anticyclone centers on Days 51-80 of January control case. Dots represent cyclones and crosses represent anticyclones. Numbers indicate additional disturbances within a cluster.

Figure 10(b) Frequency of cyclone and anticyclone centers on Days 51-80 of January ice age case. Dots represent cyclones and crosses represent anticyclones. Numbers indicate additional disturbances within a cluster.

Figure 11(a) Frequency of cyclone and anticyclone centers on Days 51-80 of July control case. Dots represent cyclones and crosses represent anticyclones. Numbers indicate additional disturbances within a cluster.

Figure 11(b) Frequency of cyclone and anticyclone centers on Days 51-80 of July ice age case. Dots represent cyclones and crosses represent anticyclones. Numbers indicate additional disturbances within a cluster.

Figure 12 Latitudinal distributions of the zonal averages of the cloud at 3 km (low cloud) for all cases. Observed data are for total cloud. January observed (A) and July observed data are from London (1957) and Van Loon (1927b). January observed (B) data are from Schutz and Gates (1971).

Figure 13 Latitudinal distribution of the zonal averages of precipitation for all cases. Observed data from Möller (1951).

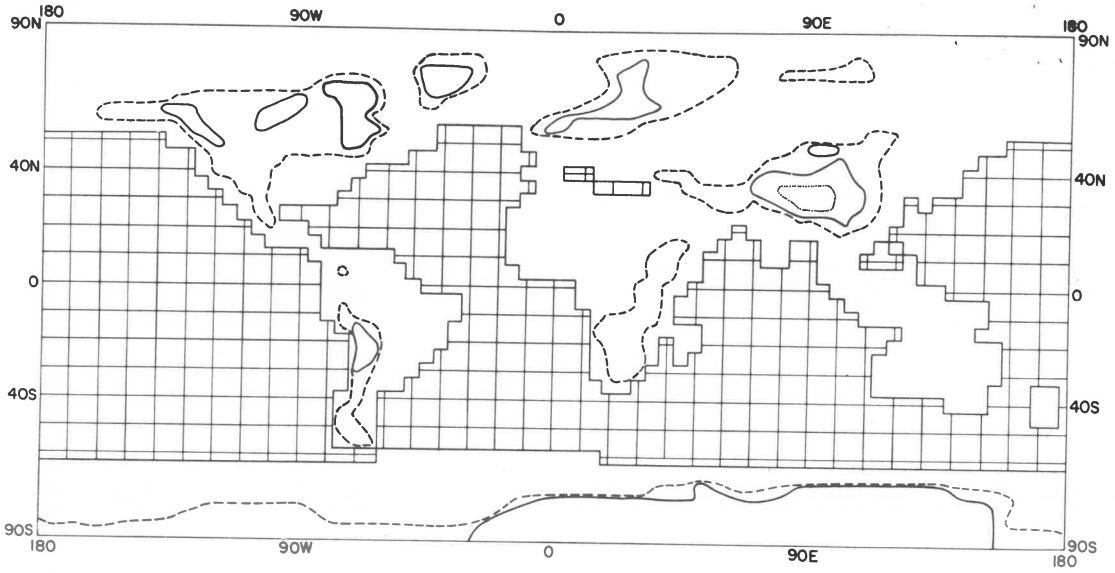

Figure 1 Outline of continents, ocean grid and orography used in January and July ice age simulations. Contours shown are: dashed line, 1 km; solid line, 2 km; dotted line, 4 km.

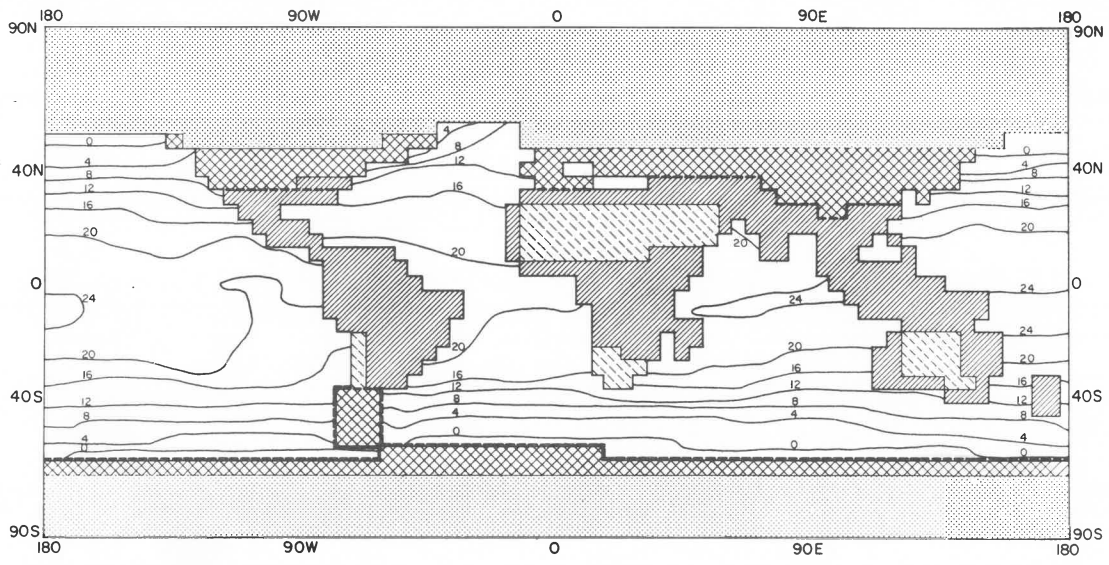

Figure 2 Albedos and sea surface temperatures used in January ice age simulation. Isotherms in °C. Dashed line is snowline. Albedos shown are: dotted, 61-100%; cross-hatched, 41-60%; [illegible]ken-hatched, 21-40%; solid-hatched, 1-20%.

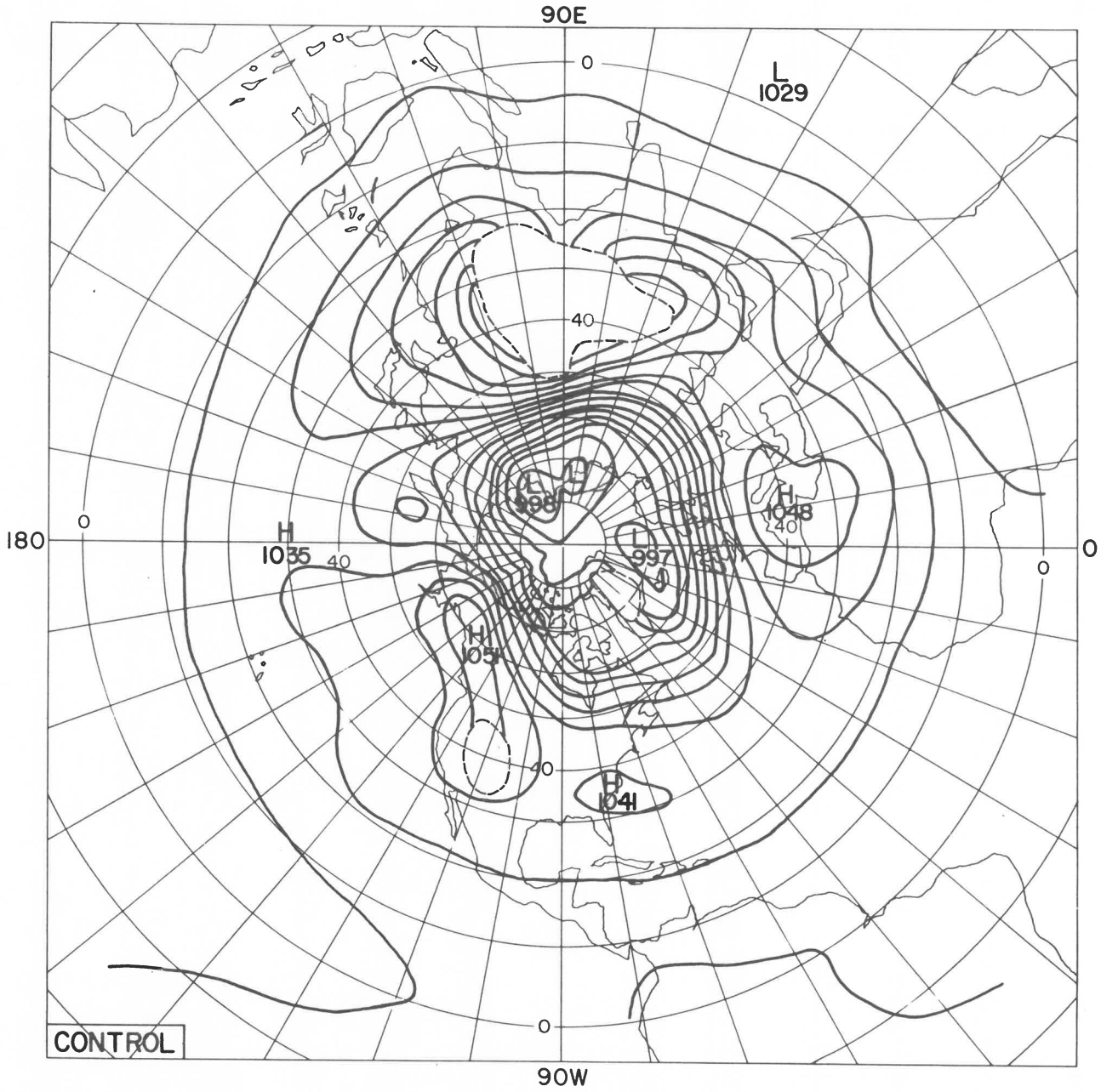

Figure 3 30-day mean pressure at sea-level for the January control case. Areas above 1.5 km outlined by dashed line.

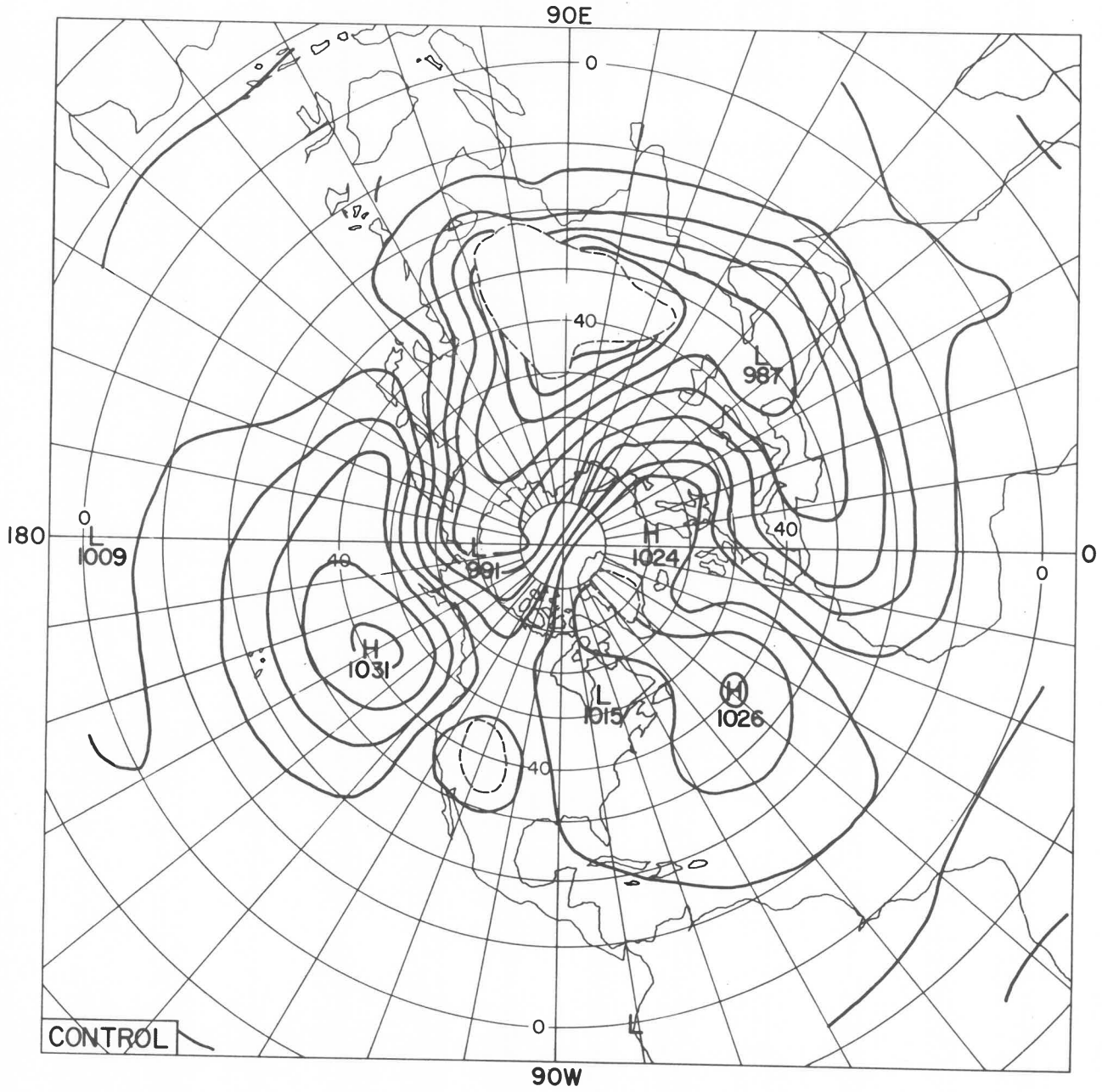

Figure 4 30-day mean pressure at sea level for the July control case. Areas above 1.5 km outlined by dashed line.

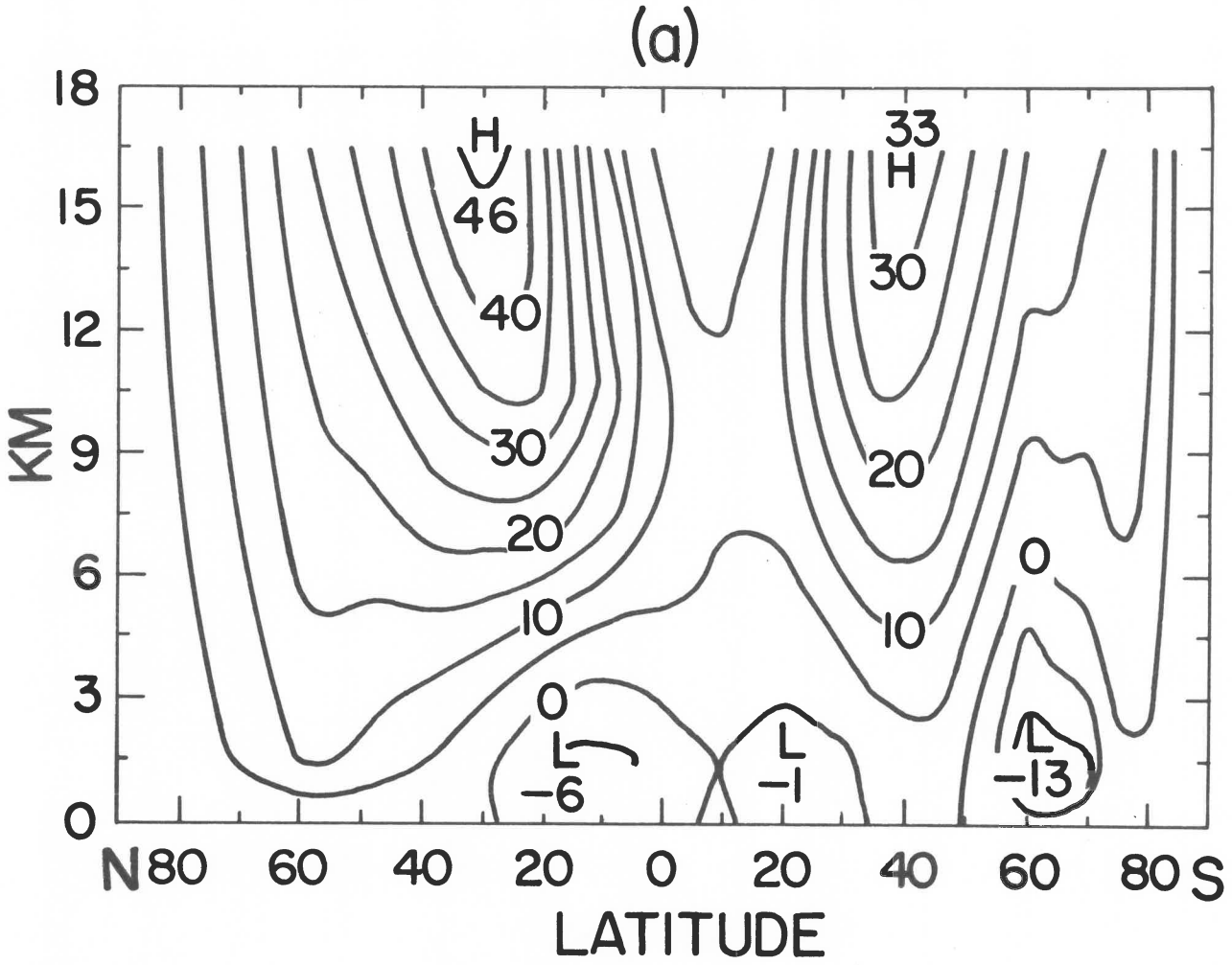

Figure 5(a) Latitude-height distribution of 30-day mean zonal wind component computed for January control case (units: m s^{-1}).

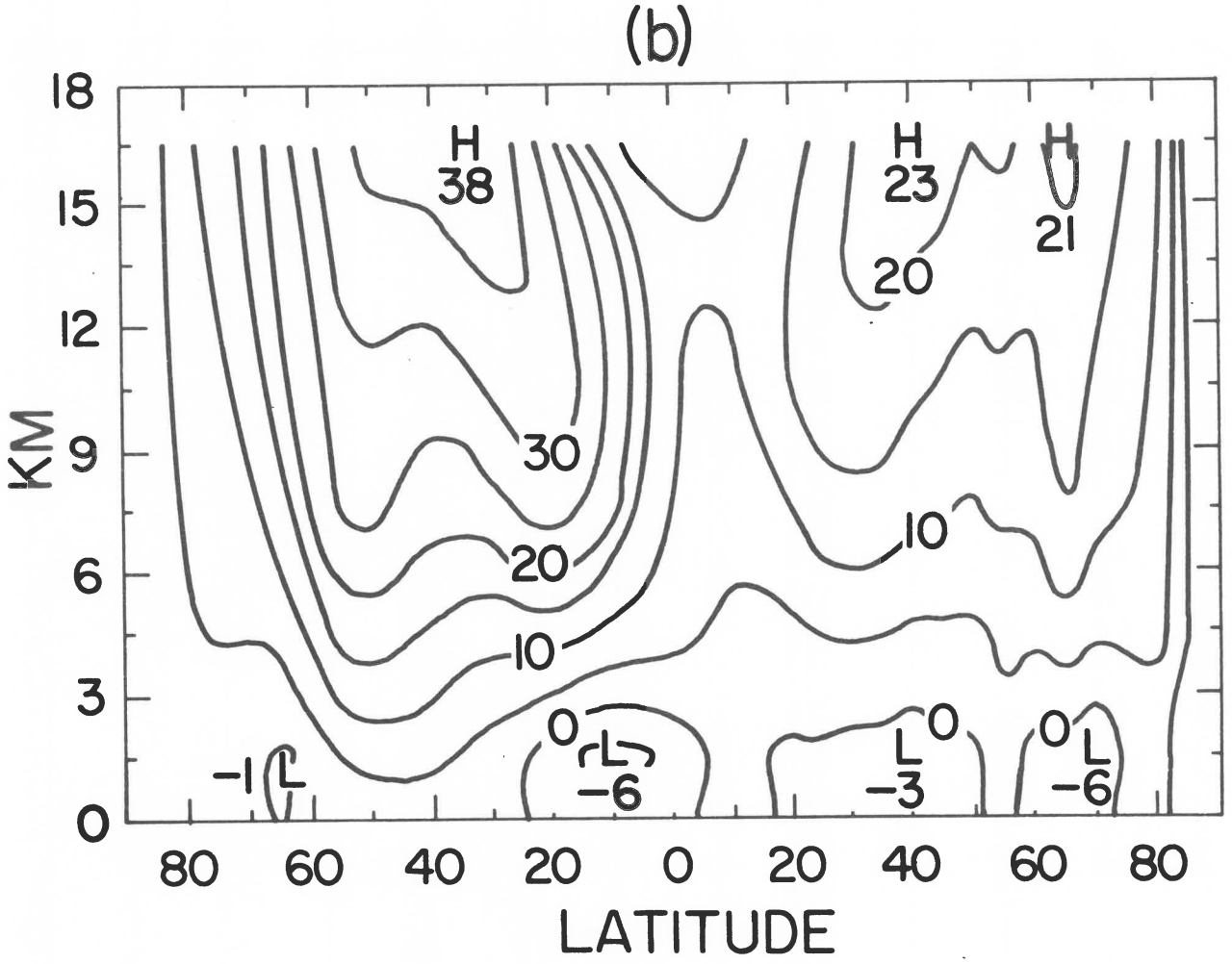

Figure 5(b) Latitude-height distribution of 30-day mean zonal wind component computed for January ice age case (units: m s^{-1}).

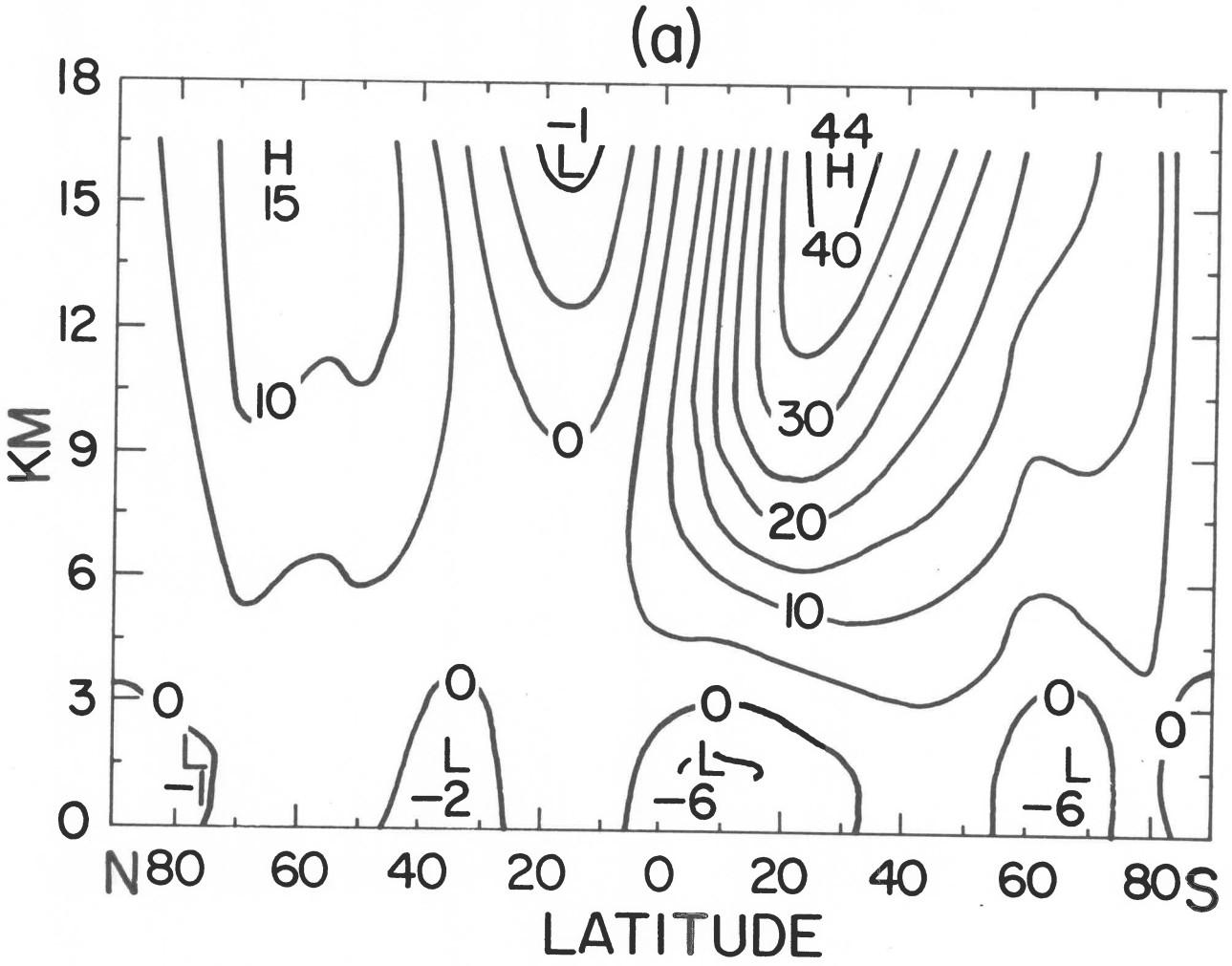

Figure 6(a) Latitude-height distribution of 30-day mean zonal wind component computed for July control case (units: m s^{-1}).

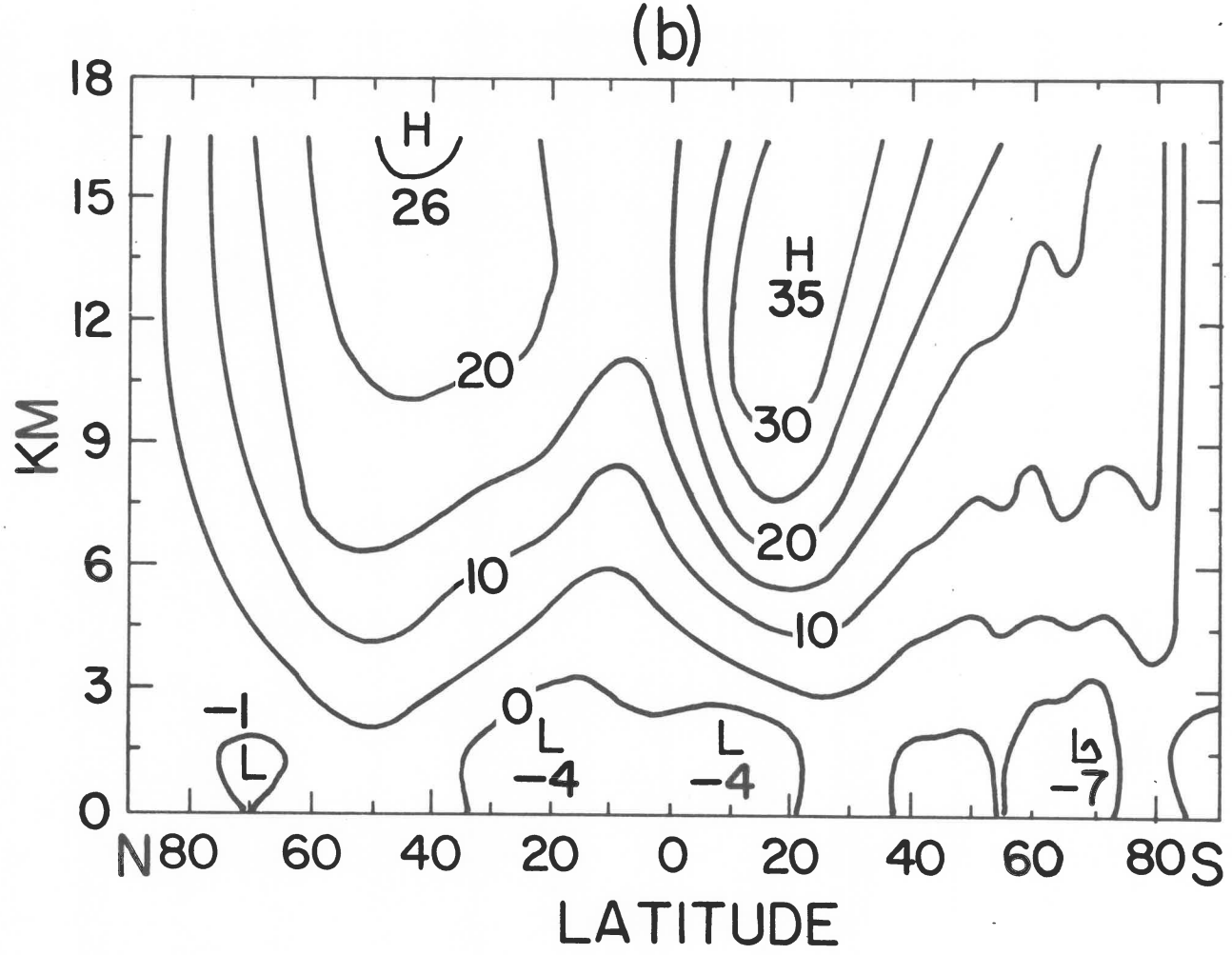

Figure 6(b) Latitude-height distribution of 30-day mean zonal wind component computed for July ice-age case (units: m s^{-1}).

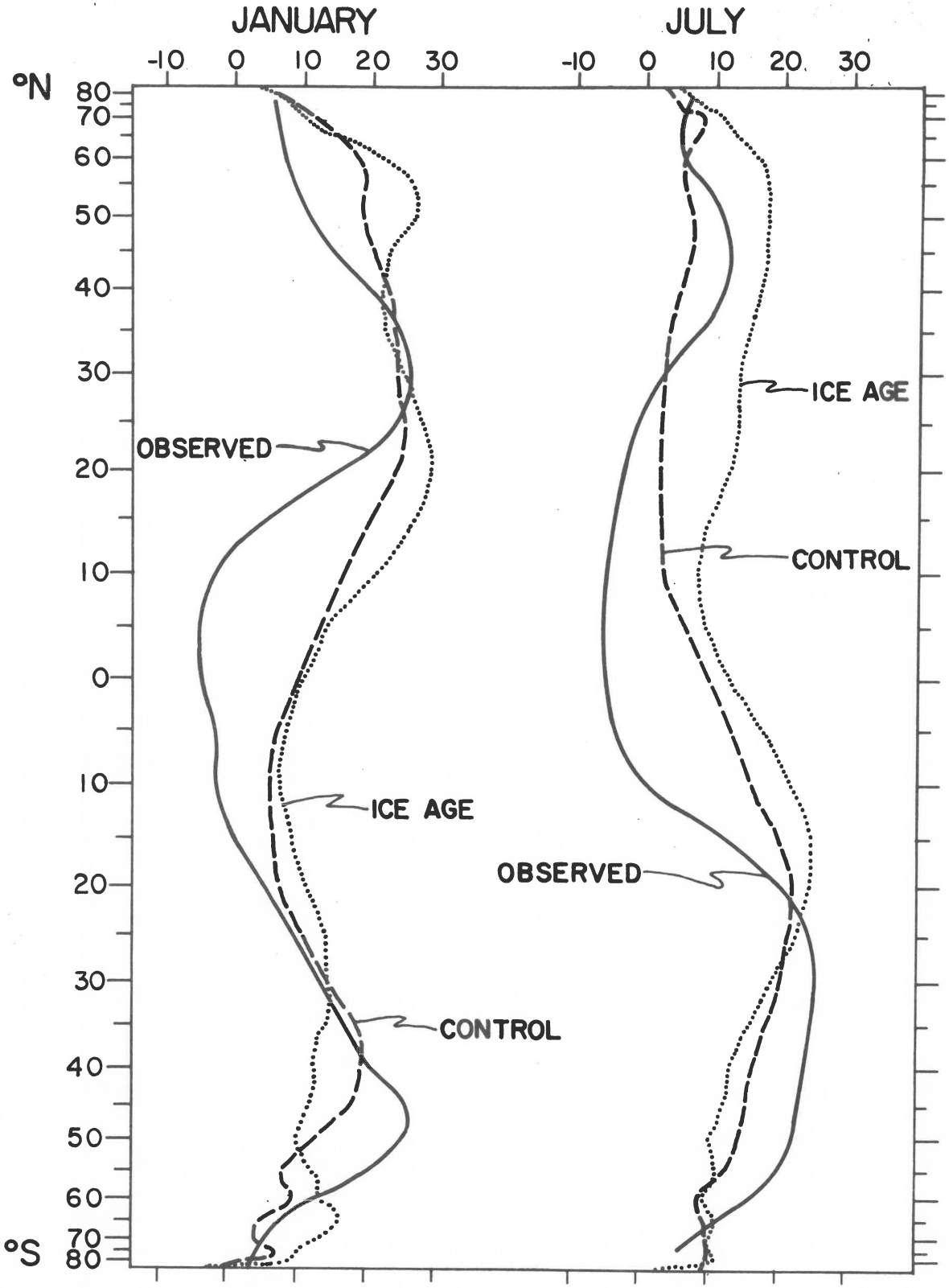

Figure 7 Latitudinal distributions of the zonal averages of the zonal wind component at 7.5 km for all cases. Observed data from Oort and Rasmusson (1971) and Van Loon (1972a).

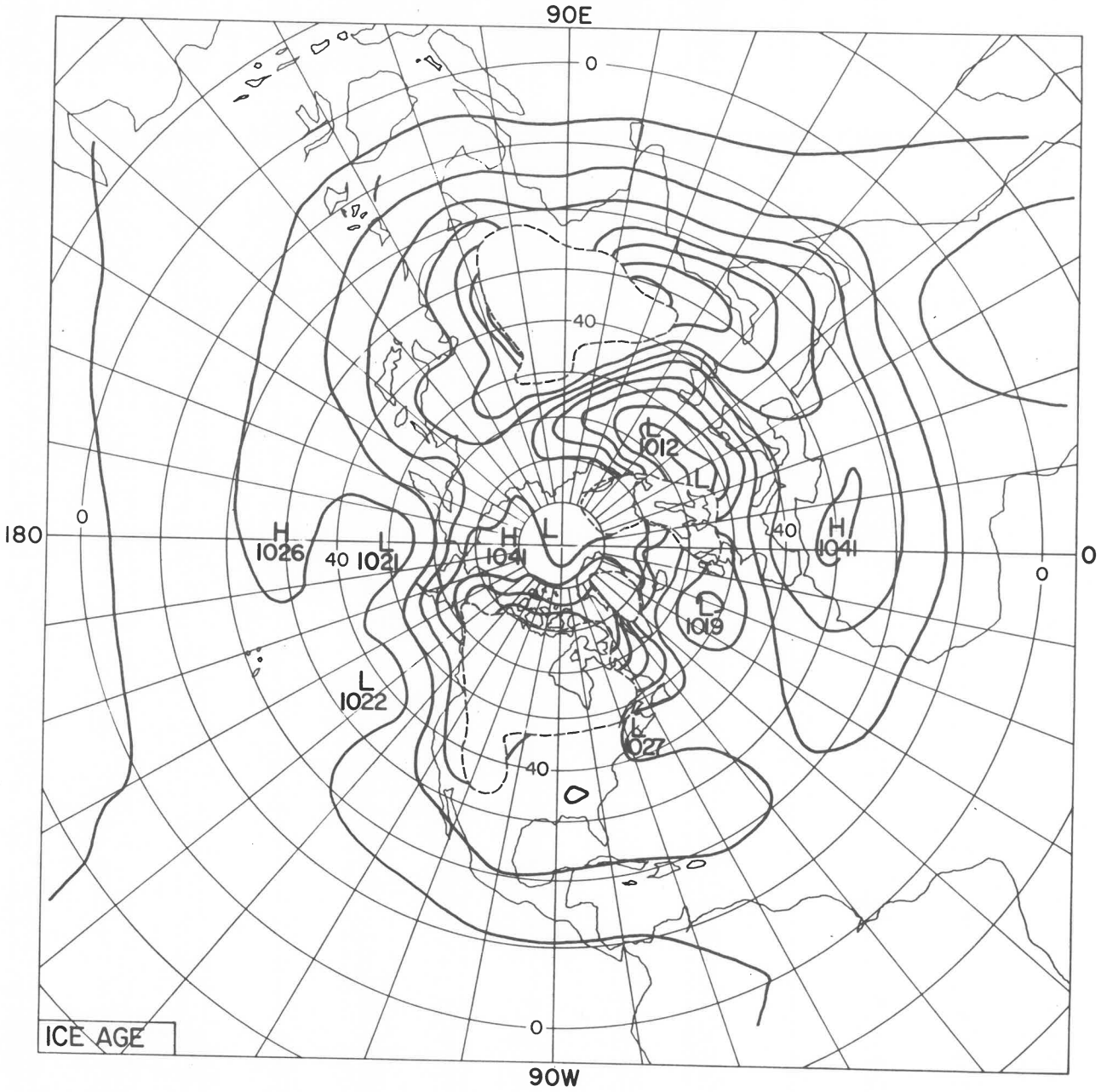

Figure 8 30-day mean pressure (mb) at sea-level for the January ice age case. Areas above 2.5 km outlined by dashed line.

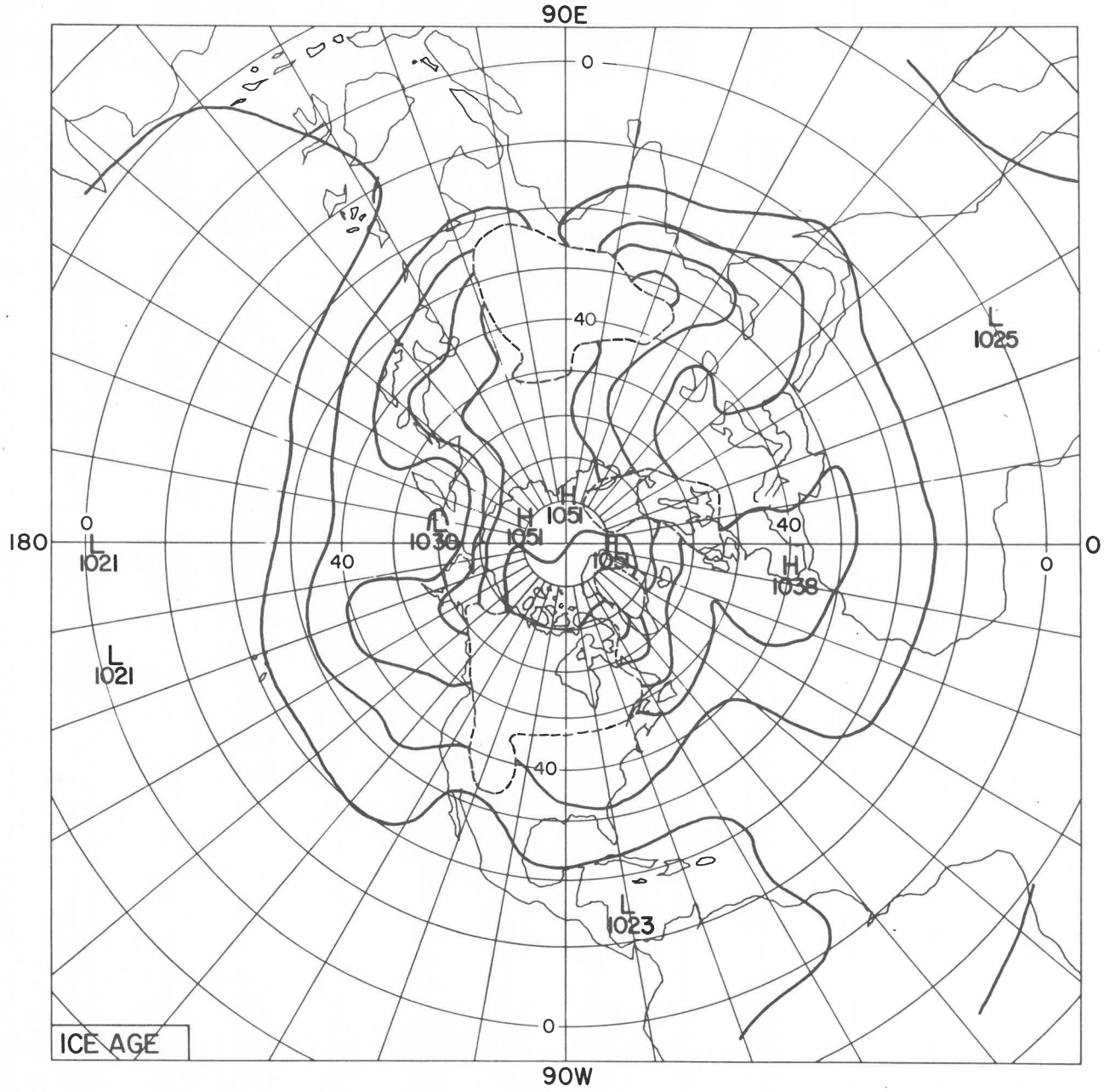

Figure 9 30-day mean pressure (mb) at sea-level for the July ice age case. Areas above 1.5 km outlined by dashed line.

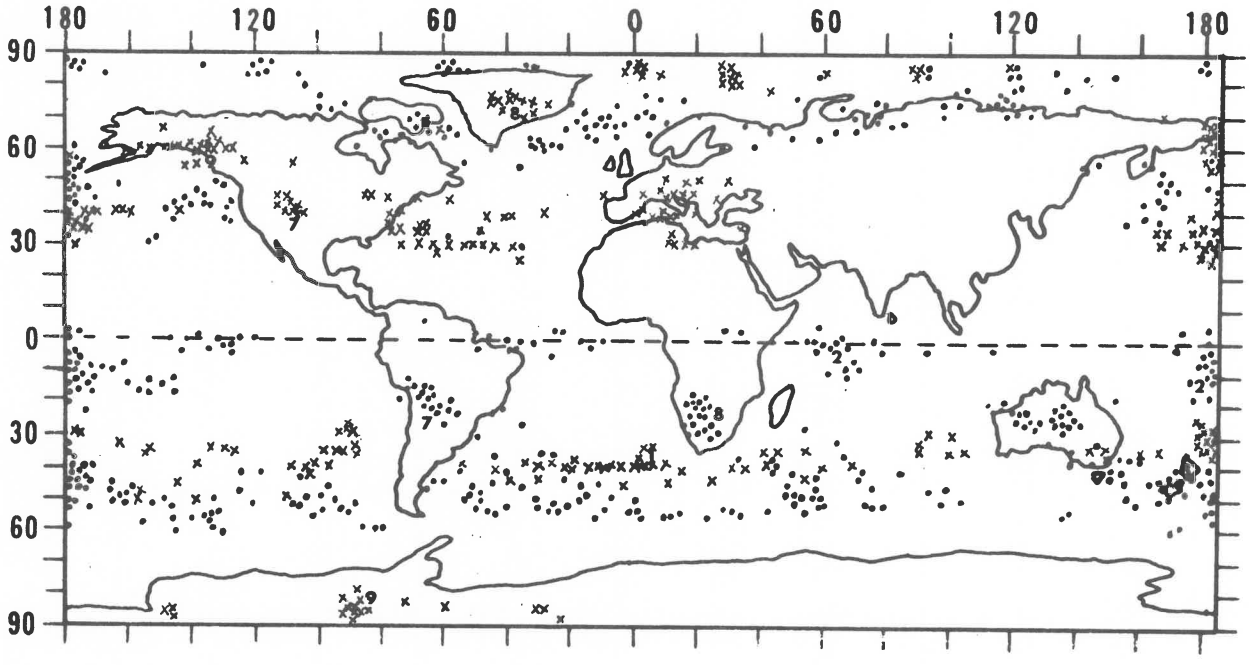

Figure 10(a) Frequency of cyclone and anticyclone centers on Days 51-80 of January control case. Dots represent cyclones and crosses represent anticyclones. Numbers indicate additional disturbances within a cluster.

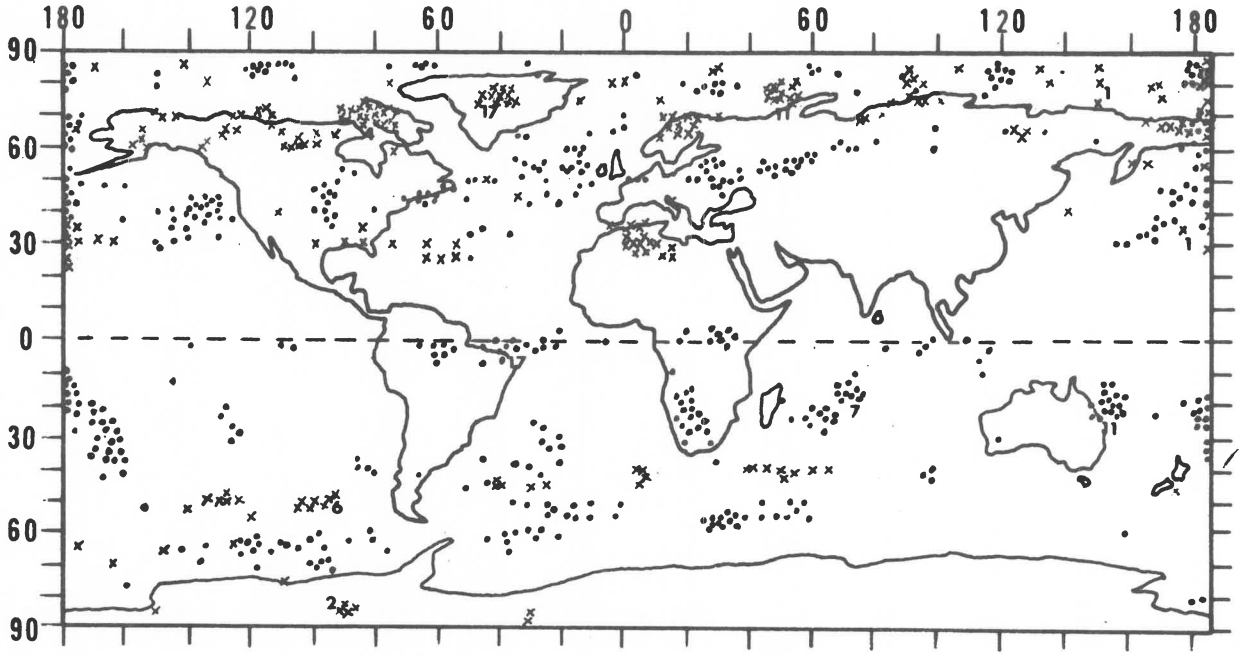

Figure 10(b) Frequency of cyclone and anticyclone centers on Days 51-80 of January ice age case. Dots represent cyclones and crosses represent anticyclones. Numbers indicate additional disturbances within a cluster.

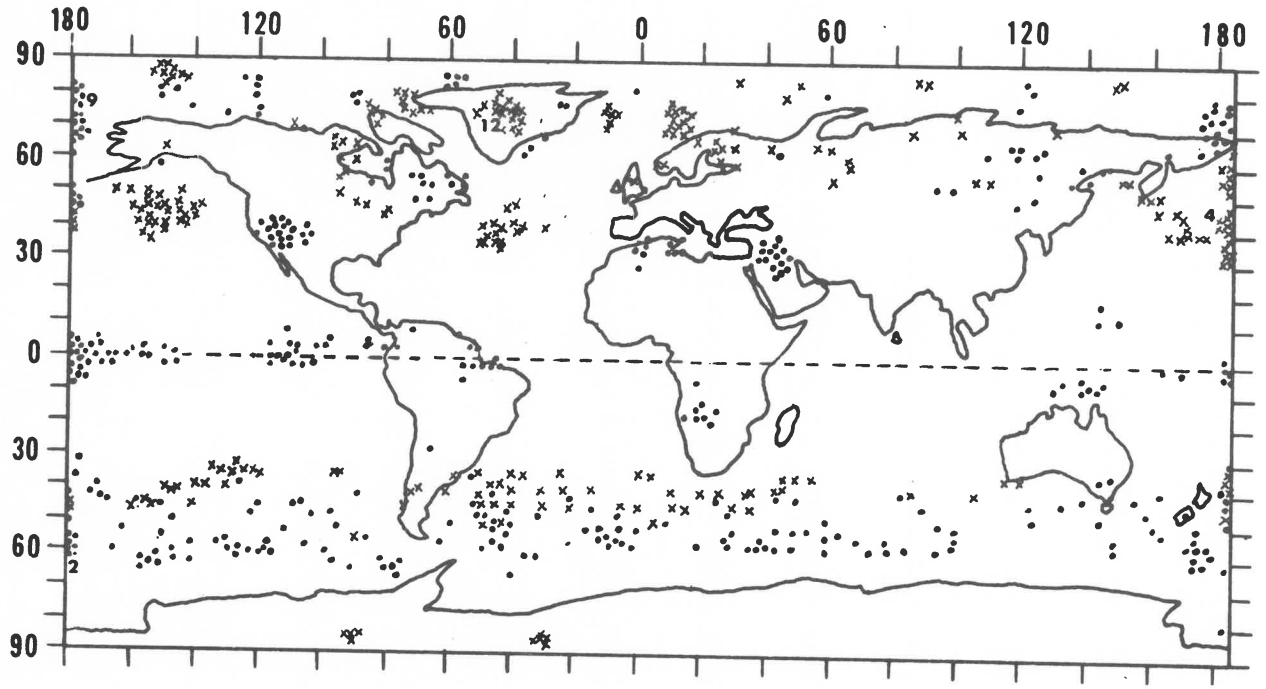

Figure 11(a) Frequency of cyclone and anticyclone centers on Days 51-80 of July control case. Dots represent cyclones and crosses represent anticyclones. Numbers indicate additional disturbances within a cluster.

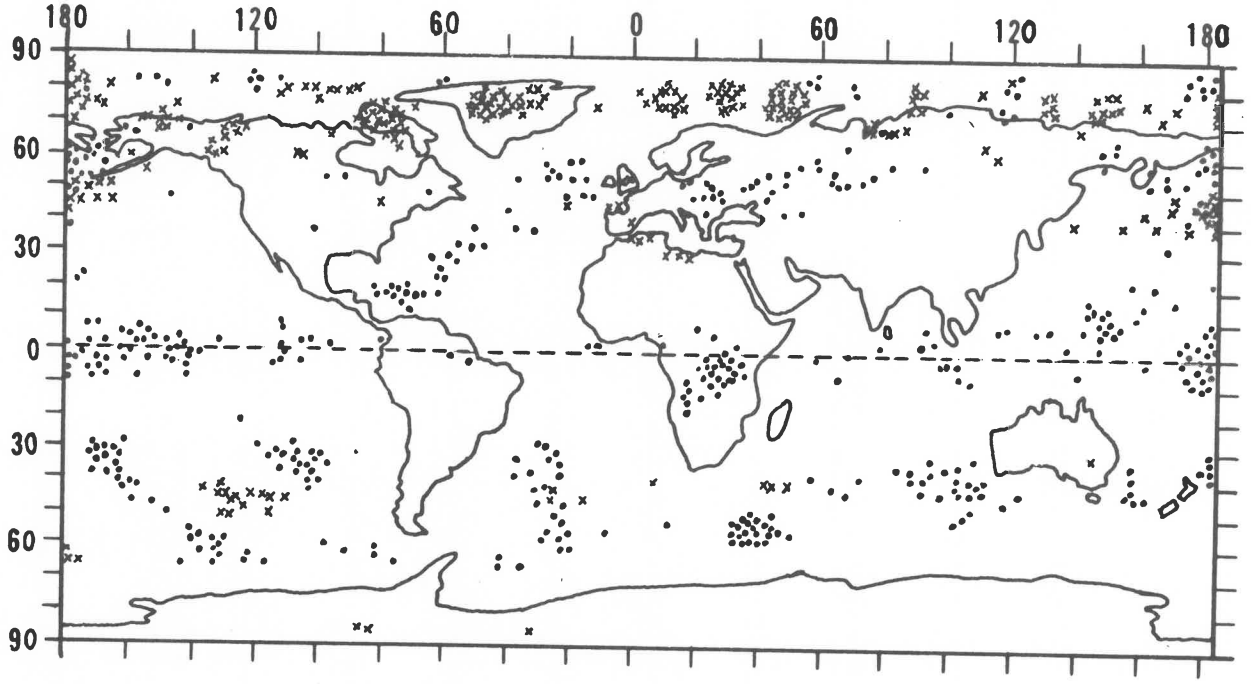

Figure 11(b) Frequency of cyclone and anticyclone centers on Days 51-80 of July ice age case. Dots represent cyclones and crosses represent anticyclones. Numbers indicate additional disturbances within a cluster.

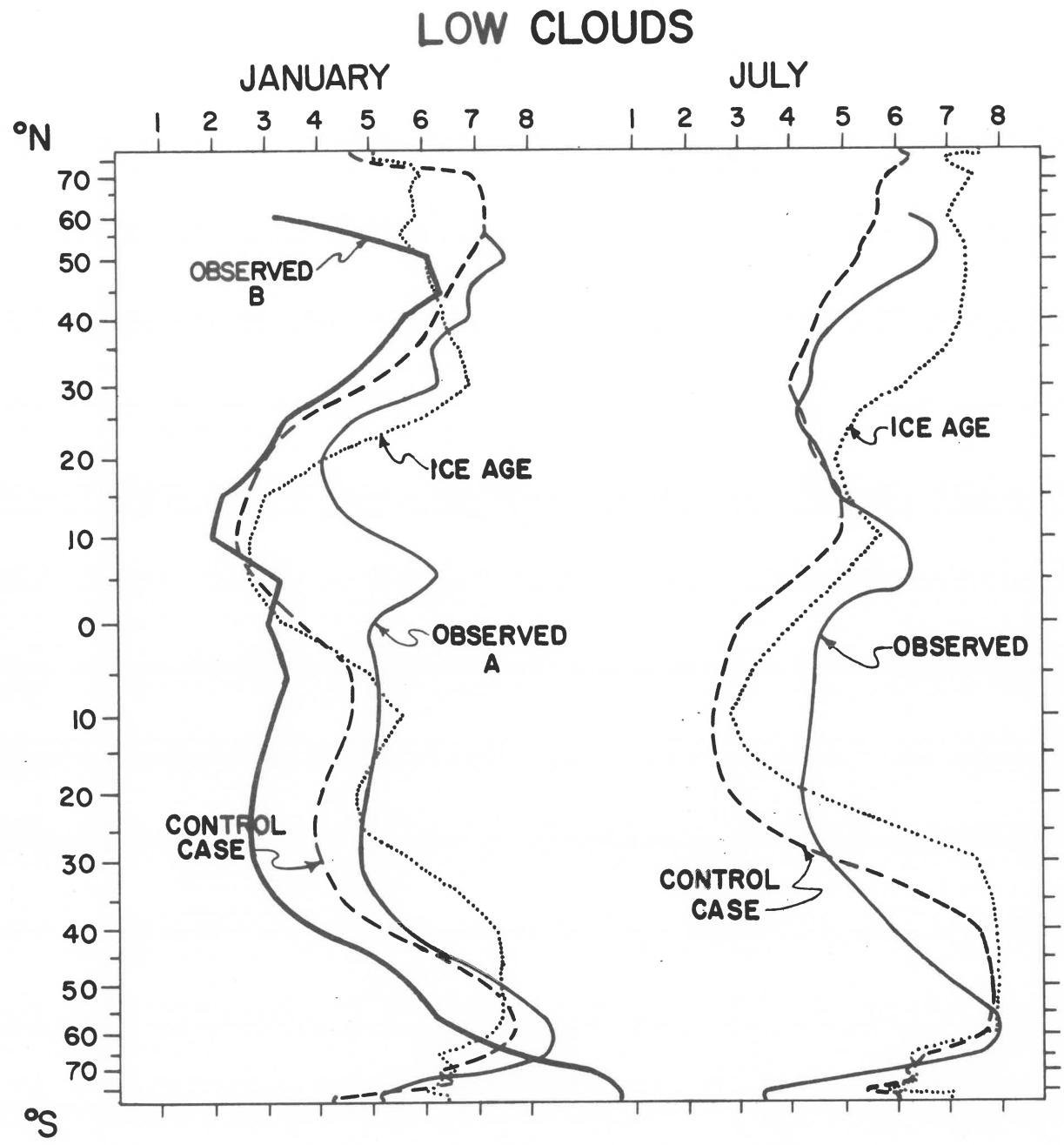

Figure 12 Latitudinal distributions of the zonal averages of the cloud at 3 km (low cloud) for all cases. Observed data are for total cloud. January observed (A) and July observed data are from London (1957) and Van Loon (1972b). January observed (B) data are from Schutz and Gates (1971).

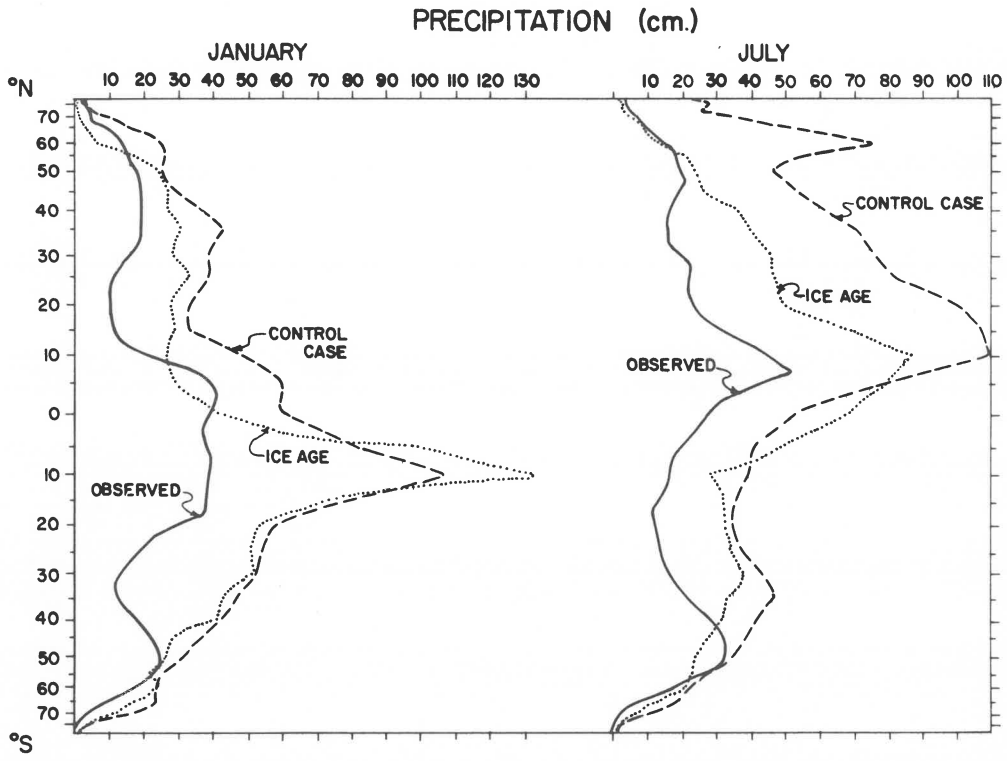

Figure 13 Latitudinal distribution of the zonal averages of precipitation for all cases. Observed data from Möller (1951).

Occasional Papers

INSTITUTE OF ARCTIC AND ALPINE RESEARCH

Occasional Paper No. 1: The Taxir Primer, R.C. Brill, 1971.

Occasional Paper No. 2: Present and Paleo-Climatic Influences on the Glacierization and Deglacierization of Cumberland Peninsula, Baffin Island, J. T. Andrews and R. G. Barry, and others, 1972.

Occasional Paper No. 3: Climatic Environment of the East Slope of the Colorado Front Range, R. G. Barry, 1972.

Occasional Paper No. 4: Short-Term Air-Sea Interactions and Surface Effects in the Baffin Bay - Davis Strait Region from Satellite Observations, J.D. Jacobs, R.G. Barry, B. Stankov and J. Williams, 1972.

Occasional Paper No. 5: Simulation of the Climate at the Last Glacial Maximum Using the NCAR Global Circulation Model, Jill Williams, R.G. Barry, and W.M. Washington, 1973.